

Figure S1 (Refers to Figure 2): **Concentration-dependent inhibition of Cytochrome B enzymatic activity by Inz-5.** Inhibition of cytochrome B enzyme activity in vitro by Inz-5 was measured as described for Figure 2. Average values from two independent experiments are depicted. Error bars indicate S.E.M.

A

Saccharomyces cerevisiae
Candida albicans
Aspergillus fumigatus
Rhizopus oryzae
Cryptococcus neoformans
Homo Sapiens

266

294

PASIV**PEWY**LLPFYAILRSIPDKLLGVIT
 PPSIV**PEWY**LLPFYAILRSIPDKLGGVIA
 PPAIV**PEWY**LLPFYAILRSIPNKLGGVIA
 PASIV**PEWY**LLPFYAILRSIPDKLGGVIA
 PPSIV**PEWY**LLPFYITILRSIPNKLGGVVG
 PPHIK**PEWY**FL**F**AYTILRS**V**PNKLGGVLA

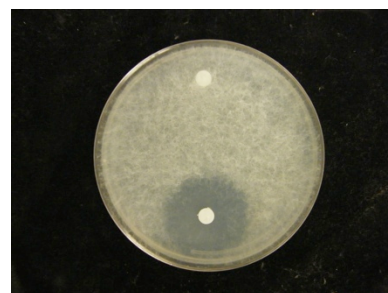
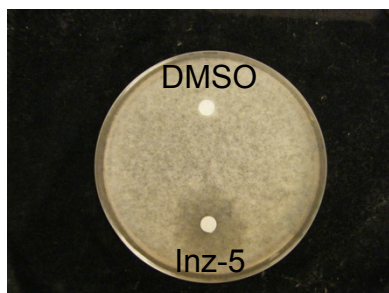
B

RPMI,
0.2% Glucose

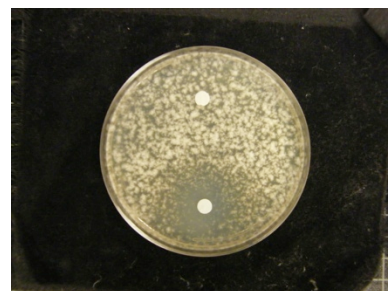
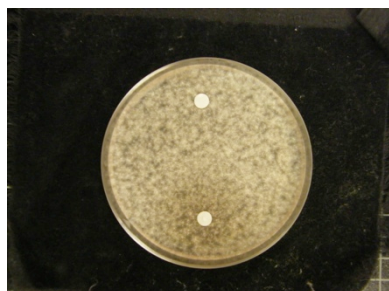
YNB,
2% Glucose

YNB,
2% Glycerol

Rhizopus
oryzae



Aspergillus
terreus



Scedosporium
prolificans

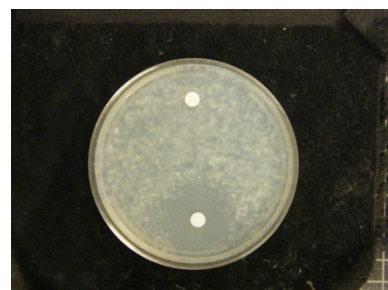
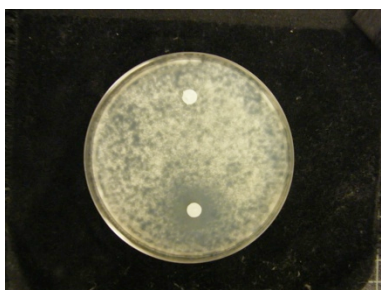
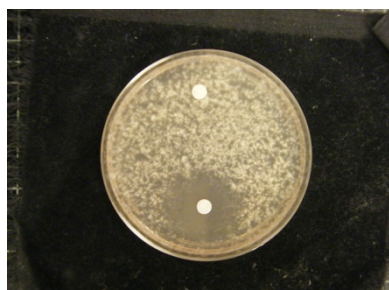
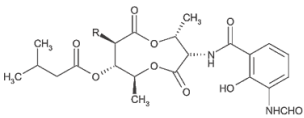
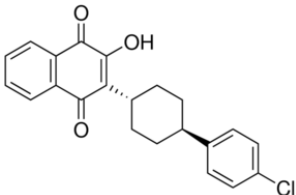
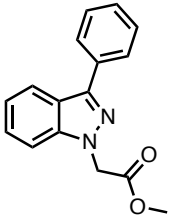
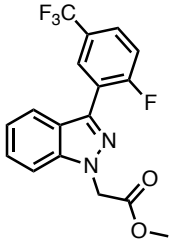
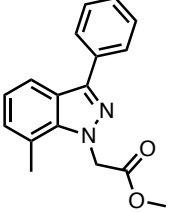
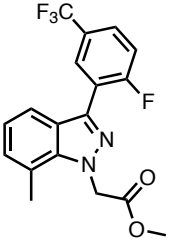
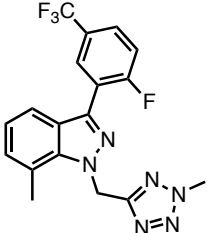
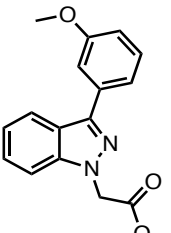
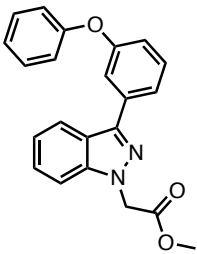
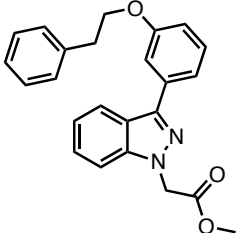
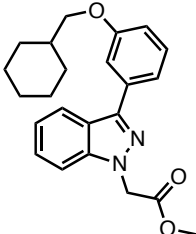
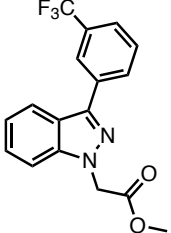
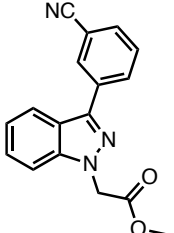


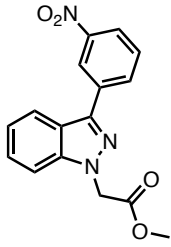
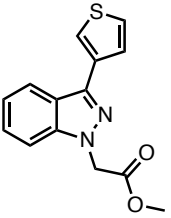
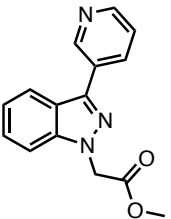
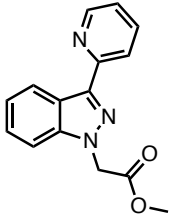
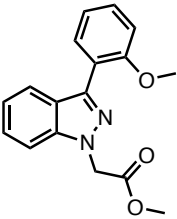
Figure S2 (Refers to Figures 5-6). **Broad spectrum activity of Inz-5.** A) Alignment of a contiguous segment within the Qo site of cytochrome bc1 from the indicated species (numbering based on *S. cerevisiae*). Mutations conferring resistance to indazoles are indicated in bold; residues conserved in all of these fungi but not humans are indicated in red. B) Activity of Inz-5 against indicated species. An ATCC reference strain for each species was grown on potato-dextrose-agar plates, then re-suspended in water with 0.1% Tween and counted by hemocytometer. Cells (104) were then plated on the indicated media with filter discs containing DMSO or 10µg Inz-5 and incubated at 35°C. Images were acquired after 24 hr (*Rhizopus*) or 48 hr (*Aspergillus* and *Scedosporium*).

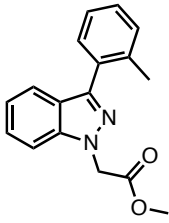
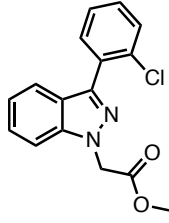
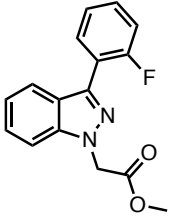
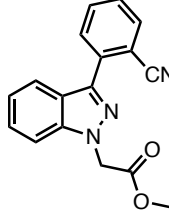
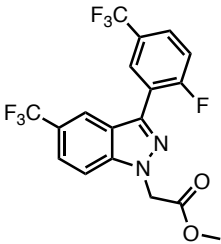
Table S1: Activities of All Compounds Tested

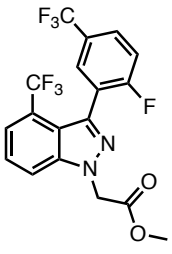
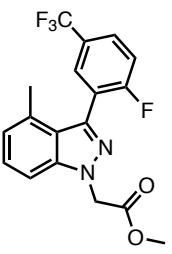
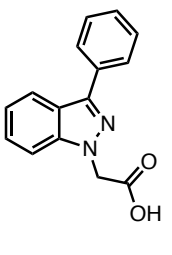
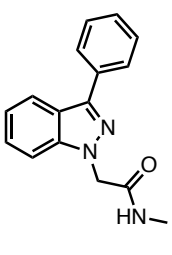
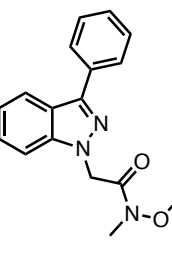
Compound Name	Structure	Candida Enzyme IC50 (μM)	Human Enzyme IC50 (μM)	Ligand Efficiency (LE)
Antimycin A		0.005	0.007	0.34
Atovaquone		3.79	1.88	0.29
Inz-1		8.092	45.32	0.36

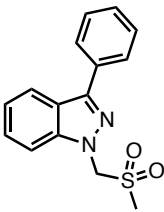
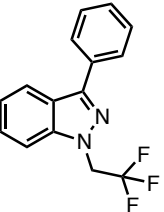
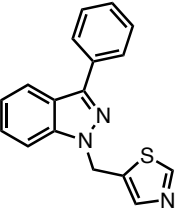
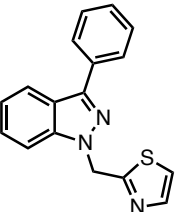
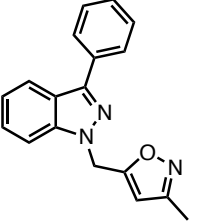
Inz-2		0.145	4.622	0.38
Inz-3		1.005	21.28	0.4
Inz-4		0.026	1.044	0.41
Inz-5		0.289	6.507	0.33
Inz-6		1.517	28.38	0.37

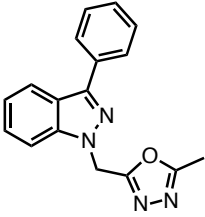
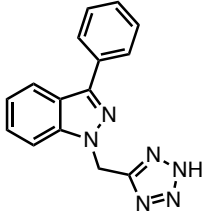
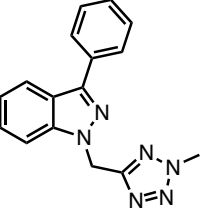
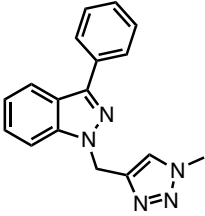
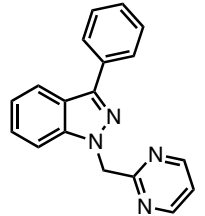
Inz-7		0.714	9.974	0.32
Inz-8		0.346	13.92	0.31
Inz-9		0.087	0.889	0.35
Inz-10		1.058	8.655	0.35
Inz-11		10.06	>64	0.32

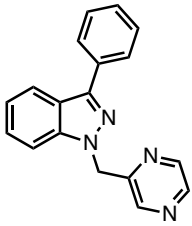
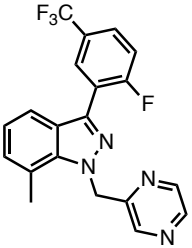
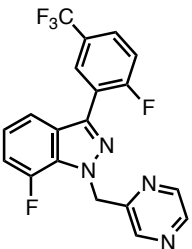
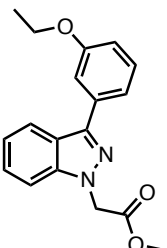
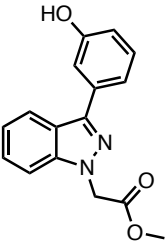
Inz-12		6.072	>64	0.32
Inz-13		9.228	>64	0.37
Inz-14		>64	>64	n.a.
Inz-15		62.38	>64	0.29
Inz-16		22.91	>64	0.3

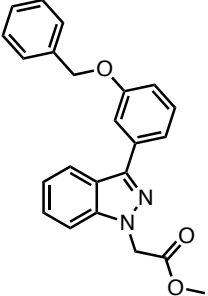
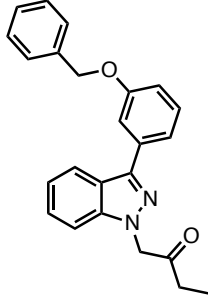
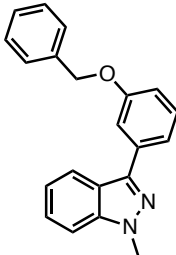
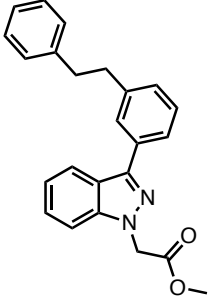
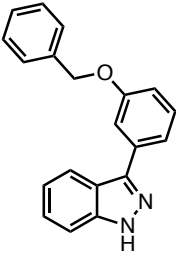
Inz-17		3.373	>64	0.37
Inz-18		5.409	>64	0.35
Inz-19		2.972	35.98	0.37
Inz-20		>64	>64	n.a.
Inz-21		>64	>64	n.a.

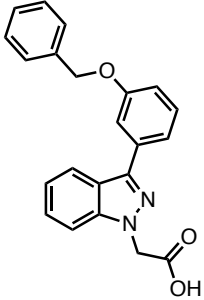
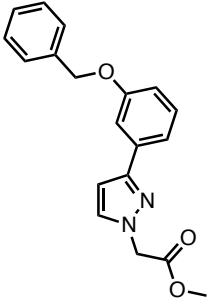
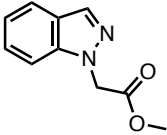
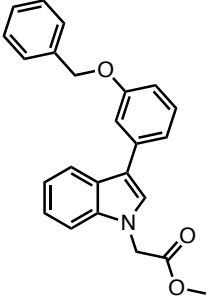
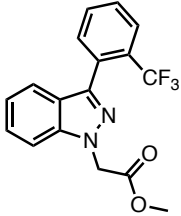
Inz-22		46.84	>64	0.21
Inz-23		10.8	>64	0.27
Inz-24		>64	>64	n.a.
Inz-25		>64	>64	n.a.
Inz-26		>64	>64	n.a.

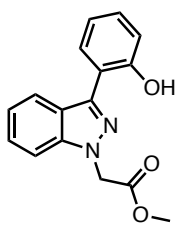
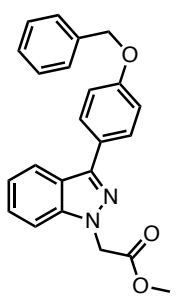
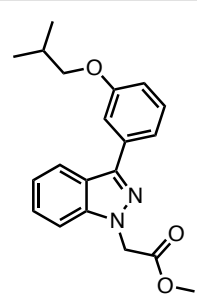
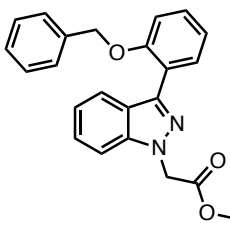
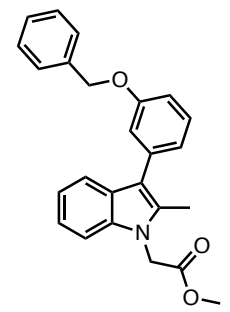
Inz-27		>64	>64	n.a.
Inz-28		>64	>64	n.a.
Inz-29		>64	>64	n.a.
Inz-30		>64	>64	n.a.
Inz-31		>64	>64	n.a.

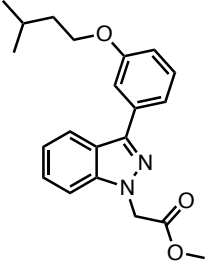
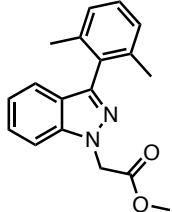
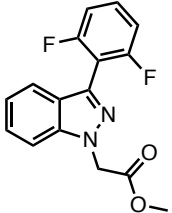
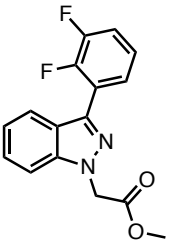
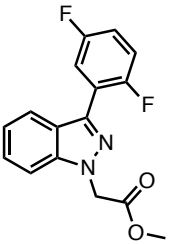
Inz-32		>64	>64	n.a.
Inz-33		>64	>64	n.a.
Inz-34		22.63	>64	0.3
Inz-35		>64	>64	n.a.
Inz-36		>64	>64	n.a.

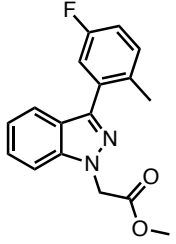
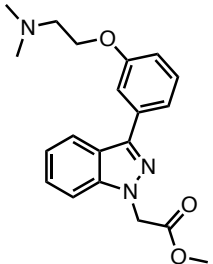
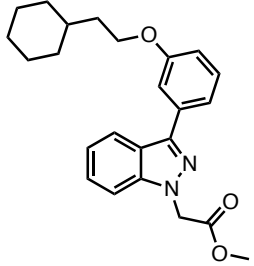
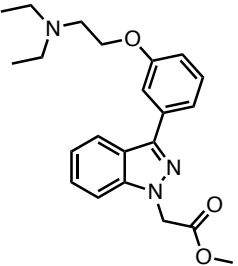
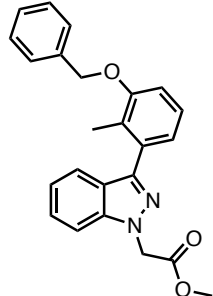
Inz-37		5.423	>64	0.34
Inz-38		0.6021	>64	0.31
Inz-39		0.141	10.78	0.34
Inz-40		0.9815	28.06	0.37
Inz-41		44.09	>64	0.29

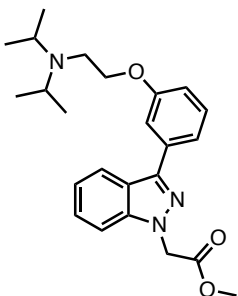
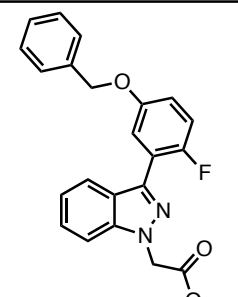
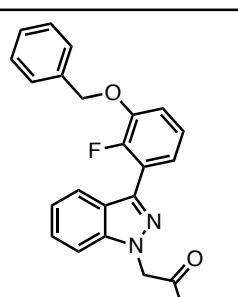
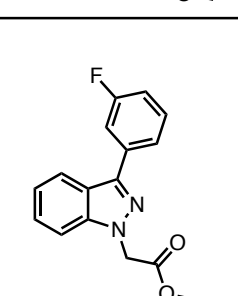
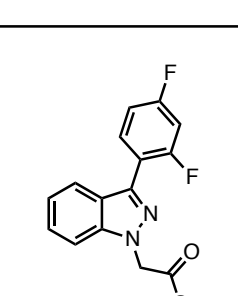
Inz-42		7.24	>64	0.26
Inz-43		22.75	>64	0.23
Inz-44		>64	>64	n.a.
Inz-45		0.06628	1.173	0.36
Inz-46		>64	>64	n.a.

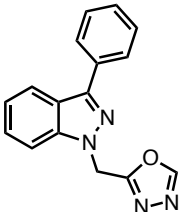
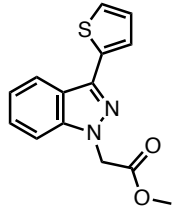
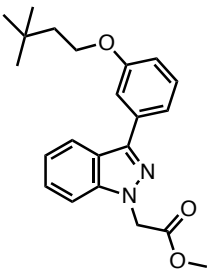
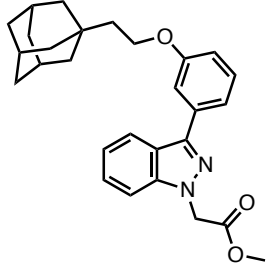
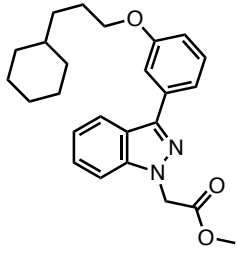
Inz-47		>64	>64	n.a.
Inz-48		>64	>64	n.a.
Inz-49		>64	>64	n.a.
Inz-50		13.13	>64	0.24
Inz-51		50.46	>64	0.25

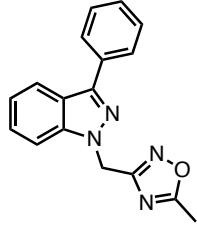
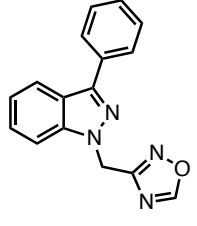
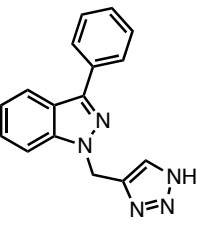
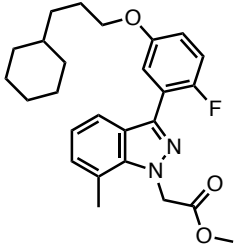
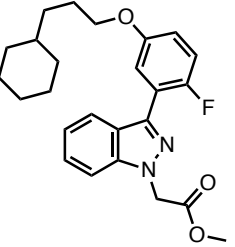
Inz-52		3.568	>64	0.36
Inz-53		43.38	>64	0.22
Inz-54		0.3444	9.232	0.36
Inz-55		>64	>64	n.a.
Inz-56		>64	>64	n.a.

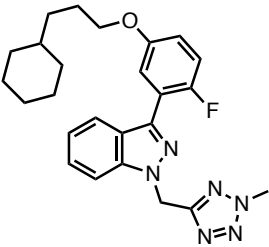
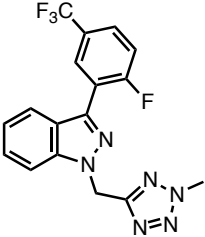
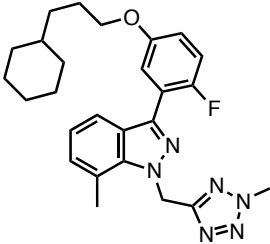
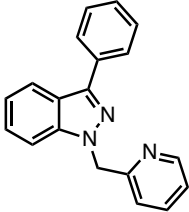
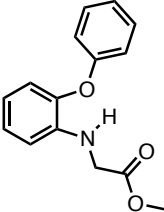
Inz-57		0.1562	4.768	0.37
Inz-58		>64	>64	n.a.
Inz-59		2.356	>64	0.36
Inz-60		1.43	>64	0.37
Inz-61		0.8908	>64	0.39

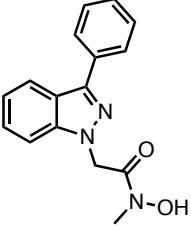
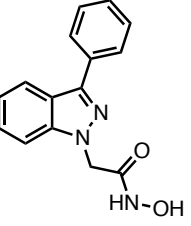
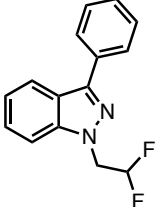
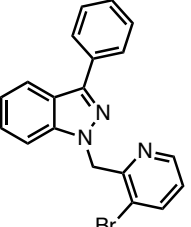
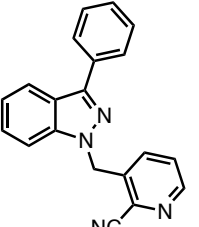
Inz-62		4.7	>64	0.34
Inz-63		35.22	>64	0.24
Inz-64		0.2999	3.234	0.32
Inz-65		13.79	>64	0.24
Inz-66		1.085	>64	0.29

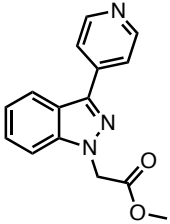
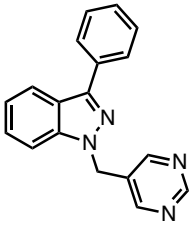
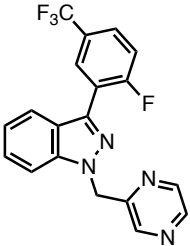
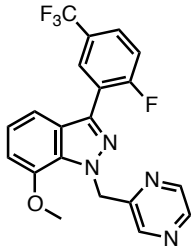
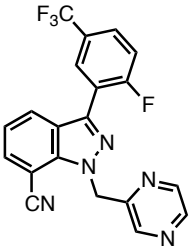
Inz-67		2.399	19.31	0.26
Inz-68		0.03516	1.664	0.36
Inz-69		3.272	>64	0.27
Inz-70		5.914	>64	0.35
Inz-71		16.64	>64	0.3

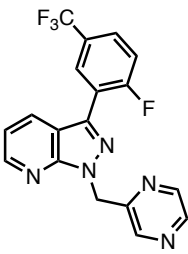
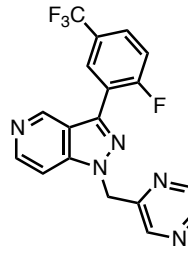
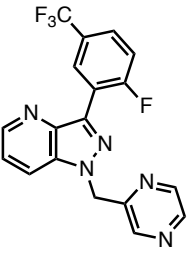
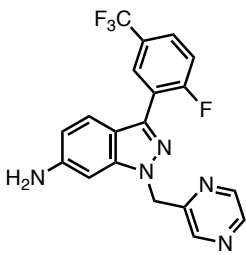
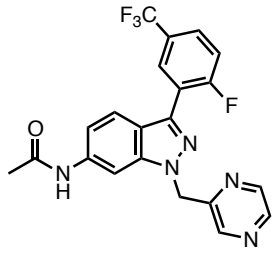
Inz-72		17.94	>64	0.32
Inz-73		15.07	>64	0.36
Inz-74		0.6568	4.715	0.32
Inz-75		1.142	1.08	0.25
Inz-76		1.795	5.465	0.27

Inz-77		>64	>64	n.a.
Inz-78		14.8	>64	0.32
Inz-79		>64	>64	n.a.
Inz-80		0.03879	0.7902	0.32
Inz-81		0.1287	2.43	0.31

Inz-82		0.6136	12.26	0.26
Inz-83		1.22	>64	0.31
Inz-84		0.1538	2.917	0.28
Inz-85		>64	>64	n.a.
Inz-86		>64	>64	n.a.

Inz-87		>64	>64	n.a.
Inz-88		>64	>64	n.a.
Inz-89		>64	>64	n.a.
Inz-90		>64	>64	n.a.
Inz-91		>64	>64	n.a.

Inz-92		>64	>64	n.a.
Inz-93		>64	>64	n.a.
Inz-94		0.4491	35.05	0.33
Inz-95		0.4375	15.19	0.31
Inz-96		22.68	>64	0.22

Inz-97		0.9354	54.39	0.31
Inz-98		20.41	>64	0.24
Inz-99		17.74	>64	0.25
Inz-100		5.482	>64	0.26
Inz-101		>64	>64	n.a.

Inz-102		>64	>64	n.a.
Inz-103		2.134	>64	0.27
Inz-104		17.58	>64	0.33

Table S1 (Refers to Figure 4). Complete list of indazoles synthesized and assayed for inhibition of yeast and human cytochrome B. All IC₅₀ determinations are average of at least 2 independent experiments which were performed as described for Figure 2. Ligand efficiency (LE) was calculated according to the following equation $1.4 * (-\log IC_{50}) / N$, where N is the number of heavy atom (non-hydrogen atoms). n.a. stands for “not applicable”.

Compound name	Structure	<i>Candida</i> Enzyme IC ₅₀ (μM)	Human Enzyme IC ₅₀ (μM)	Ligand Efficiency (LE)
Inz-1		8.092	45.320	0.36
Inz-6		1.517	28.380	0.37
Inz-7		0.714	9.974	0.32
Inz-8		0.346	13.920	0.31
Inz-9		0.087	0.889	0.35
Inz-10		1.058	8.655	0.35
Inz-11		10.060	>64	0.32
Inz-12		6.072	>64	0.32

Compound name	Structure	<i>Candida</i> Enzyme IC ₅₀ (μM)	Human Enzyme IC ₅₀ (μM)	Ligand Efficiency (LE)
Inz-13		9.228	>64	0.37
Inz-14		>64	>64	n.a.
Inz-15		62.340	>64	0.29
Inz-16		22.910	>64	0.30
Inz-17		3.373	>64	0.37
Inz-18		5.409	>64	0.35
Inz-19		2.972	35.980	0.37
Inz-20		>64	>64	n.a.
Inz-2		0.144	4.622	0.38

Table S2 (refers to Figure 4). Summary of the SAR study relative to the top aromatic ring.

Compound name	Structure	<i>Candida</i> Enzyme IC ₅₀ (μM)	Human Enzyme IC ₅₀ (μM)	Ligand Efficiency (LE)
Inz-1		8.092	45.320	0.36
Inz-21		>64	>64	n.a.
Inz-22		46.840	>64	0.21
Inz-23		10.800	>64	0.27
Inz-3		1.005	21.280	0.40
Inz-2		0.144	4.622	0.38
Inz-4		0.026	1.044	0.41

Table S3 (refers to figure 4). Summary of the SAR study relative to the indazole core.

Compound name	Structure	<i>Candida</i> Enzyme IC ₅₀ (μM)	Human Enzyme IC ₅₀ (μM)	Ligand Efficiency (LE)
Inz-1		8.092	45.320	0.36
Inz-24		>64	>64	n.a.
Inz-25		>64	>64	n.a.
Inz-26		>64	>64	n.a.
Inz-27		>64	>64	n.a.
Inz-28		>64	>64	n.a.
Inz-29		>64	>64	n.a.
Inz-30		>64	>64	n.a.
Inz-31		>64	>64	n.a.

Compound name	Structure	<i>Candida</i> Enzyme IC ₅₀ (μM)	Human Enzyme IC ₅₀ (μM)	Ligand Efficiency (LE)
Inz-32		>64	>64	n.a.
Inz-33		>64	>64	n.a.
Inz-34		22.630	>64	0.30
Inz-35		>64	>64	n.a.
Inz-36		>64	>64	n.a.
Inz-37		5.423	>64	0.34
Inz-38		0.6021	>64	0.31
Inz-39		0.141 (0.758) ^(a)	10.78 (12.980) ^(b)	0.34 (17) ^(c)
Inz-5		0.289 (0.381)^(a)	6.507 (10.590)^(b)	0.33 (28)^(c)

(a) *Candida* Growth IC₅₀ (μM). (b) HepG2 Respiring Growth IC₅₀ (μM).

(c) Selectivity (HepG2/ *Candida*).

Table S4 (refers to figure 4). Summary of the SAR study relative to the replacement of the methyl ester group.

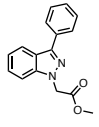
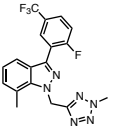
Compound	Structure	Plasma stability (%Remaining material after an incubation of 1 hr)	Microsome stability (% Remaining material after 15 min incubation without NADPH) ^c	Microsome stability (% Remaining material after 15 min incubation with NADPH) ^d
Inz-1		0	0	0
Inz-5		100 (100) ^b	50	19.5

Table S5 (refers to figure 4). Plasma and Microsomal stability of Inz-1 and Inz-5.

SUPPLEMENTAL EXPERIMENTAL PROCEDURES

High throughput screening hit triage: Inz-1

We queried the pubchem database with a substructure search using the structure of our original screening hit, Inz-1. Inz-1 was tested in 801 bioassays (run by other investigators through the MLPCN program) and appeared as a hit in 5 of them (0.62%). Inz-1 was confirmed as a hit in 2 of these assays (Bioassay AID 2147, qHTS Assay for Inhibitors of Human Jumonji Domain Containing 2E, EC50 28.18 μM ; Bioassay AID 434955, Screen to Identify Novel Compounds that Sensitize Mycobacterium Tuberculosis to Beta-lactam Antibiotics, IC90 100 μM); and a primary screen hit (not confirmed at dose) in 3 other assays: Screening for Modulators of Post-Golgi Transport, Control Strain (AID 738), Allosteric Modulators of D1 Receptors, Primary Screen (AID 641), and uHTS Luminescent assay for identification of inhibitors of NALP3 in yeast (AID 2825). Inz-1 was not pursued as a hit by the investigators in any of these screens. We determined that the activity of Inz-1 in AID 738 and AID 2071, two yeast-based whole-cell assays, was likely to be an on-target effect due to inhibition of mitochondrial respiration by Inz-1.

Cytochrome B Structural Alignment and Docking of Indazoles *in silico*

Cytochrome bc1 from *Saccharomyces cerevisiae* (PDB: 1P84) was aligned to cytochrome bc1 from *Bos taurus* (PDB: 1SQV), using the “align structures” feature in Pymol (www.pymol.org). Ligands were docked into the active site using the GLIDE package (Schrodinger suite). The initial unbound ligand conformation was generated using SMILES sequences, which were converted to a 3D structure using Ligprep (Schrodinger Suite). For docking, the native ligand, ubiquinol, was removed from the active site of the crystal structure (PDB Code: 1EZV). A grid of 16Å was generated centered on the active site. To generate an improved bound conformation, we used an inverse design approach, which has been described in detail before (Altman et al., 2008; Huggins et al., 2009). In short, an ensemble of scaffold conformations is generated in the active site, with appropriate attachment points for the functional groups. The top docked conformation of Inz-1 was used to generate an initial conformation for the scaffold. We thoroughly sampled in both translation and rotation throughout the active site to generate an ensemble of possible scaffold positions. We further sampled the bond between the indazole and the benzene every degree (Bond shown in green). We rotamerized the functional group by enumerating all dihedrals every 30 degrees and employed a Dead-end Elimination/A* approach, which guarantees the global minimum energy conformation. Finally, we rescored the top conformations using an energy model with increased accuracy as previously described (Huggins et al., 2009).

Plasma and microsome stability profiling

Inz-1 and Inz-5 were incubated at 1 μM in 100mM potassium phosphate buffer, pH 7.4, with 0.5mg/mL CD-1 mouse microsomes or plasma in the presence or absence of 1mM NADPH. Imatinib was used as an internal control. At various time points, acetonitrile was added to terminate the reaction and extract the compounds, which were quantitated using a Thermo Scientific QExactive Orbitrap UPLC/MS/MS.

Fungal growth, strain manipulation, drug treatment and MIC assays

Phenotypic profiling experiments were performed in 96-well flat-bottom plates by diluting overnight YPD cultures to a starting OD of 0.0003, then assaying growth in drug and stress conditions after 24 or 48 hours (as indicated) by reading OD600. In these experiments, drugs and concentrations included 0.9M NaCl, 0.05 $\mu\text{g}/\text{mL}$ aureobasidin, 80 μM bathophenanthroline disulfonic acid, 0.5 $\mu\text{g}/\text{mL}$ cerulenin, 2mM tert-butyl peroxide, 40 mg/L calcofluor white, 2 $\mu\text{g}/\text{mL}$ tunicamycin, 0.1 $\mu\text{g}/\text{mL}$ caspofungin, 25 μM simvastatin, and 0.008% SDS. Small molecule inhibitor drugs were used at either 2.5 μM (Brefeldin A), 5 μM (Geldanamycin, FK-506, cercosporamide), 10 μM (Trichostatin A, Inz-1), 15 μM (MDL-12,330A), or 20 μM (rotenone). Synthetic media used a base of Difco Yeast-Nitrogen-Base (YNB) with complete amino acid supplement, and addition of 2% glucose or 2% glycerol. Growth results were quantitatively displayed in heatmaps using Treeview as described previously (Vincent et al., 2013). Minimal inhibitory concentration (MIC) assays were performed at 2 fold concentration increments in 96-well plates over 24-72 hours as described in figure legends. The MIC was defined as the lowest concentration that results in no visible fungal growth.

SUPPLEMENTAL CHEMICAL SYNTHESIS PROCEDURES

General reagent information

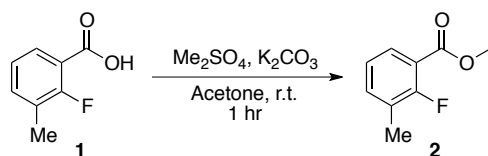
Commercial materials were purchased and used as received unless otherwise noted. Acetonitrile (anhydrous, 99.8%) and *N,N*-dimethylformamide (anhydrous, 99.8%) were purchased from Sigma-Aldrich. Acetone (ACS reagent, 99.6%) was purchased from Acros Organics. Tetrahydrofuran was purified and dried using a solvent purification system consisting of successive passage through alumina and Q5 reactant-packed columns.

Deionized water was employed; this solvent was degassed by sonication under slight vacuum for 5 minutes, followed by backfilling with argon. Potassium carbonate (ACS reagent, 99.0%), tribasic potassium phosphate (reagent grade, 98%) and sodium azide (ReagentPlus®, 99.5%) were purchased from Sigma-Aldrich. Ammonium chloride (ACS reagent, 99.6%) was purchased from Acros Organics. Phosphorus (V) oxychloride (ReagentPlus®, 99%), hydrazine monohydrate (N₂H₄ 64-65%, reagent grade, 98%), bromoacetonitrile (97%) and dimethylsulfate (99%) were purchased from Sigma-Aldrich. (Trimethylsilyl)diazomethane solution (2M in hexanes) was purchased from Sigma-Aldrich and kept in a fridge at -5 °C. 2-fluoro-5-(trifluoromethyl)-phenylboronic acid was purchased from Combi-Blocks. 2-fluoro-3-methylbenzoic acid was purchased from Oakwood Chemicals. XPhos ligand was purchased from Strem and precatalyst **P** was prepared following a reported procedure. (Kinzel et al., 2010) Compounds described herein were purified by flash chromatography using Silicycle SiliaFlashP60 (230-400 mesh) silica gel.

General analytical information

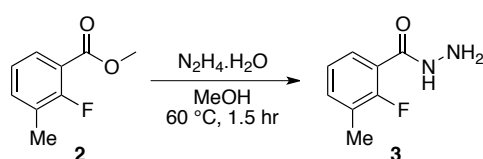
All compounds described herein were characterized by ¹H, ¹³C and ¹⁹F NMR (when applicable). ¹H, ¹³C and ¹⁹F NMR spectra were recorded on Brüker 400 MHz spectrometers. The samples were prepared in CDCl₃, and chemical shift (δ) are given in parts per million (ppm) relative to the residual solvent peak (7.26 ppm for ¹H and 77.16 ppm for ¹³C). Few samples were prepared in d⁶-DMSO (2.50 ppm for ¹H and 39.51 ppm for ¹³C). ¹⁹F NMR were performed with proton decoupling. Peak multiplicity is reported as: s (singlet), d (doublet), t (triplet), q (quartet), m (multiplet), dd (doublet of doublets), dt (doublet of triplets), ddd (doublet of doublets of doublets), td (triplet of doublets), br (broad), app (apparent). Coupling constants (*J*) are given in Hertz (Hz). Mass spectrometry analysis was performed for **Inz-5**. HRMS data were obtained using a direct analysis in real time (DART) ionization method on a Brüker Daltonics APEXIV 4.7 Tesla Fourier Transform Ion Cyclotron Resonance Mass Spectrometer (FT-ICR-MS). The relative purity of **Inz-5** was determined using LC-MS analysis on an Agilent 1260 Infinity Chromatograph coupled with an Agilent 6120 Quadrupole Mass detector. The analyses were performed using an Eclipse XDB-C18 column (5 μm, 4.6x150 mm) using an isocratic mobile phase composed of 90% of acetonitrile, 9.9% of water and 0.1% of acetic acid (flow rate = 0.8 ml/min).

Preparation of Inz-5



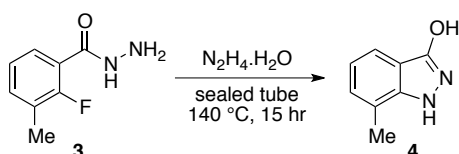
Scheme 1. Preparation of methyl 2-fluoro-3-methylbenzoate **2**.

Methyl 2-fluoro-3-methylbenzoate 2: 2-fluoro-3-methylbenzoic acid **1** (2 g, 13 mmol, 1 eq) was charged into a 100-ml round-bottomed flask and dissolved in acetone (20 ml). Potassium carbonate (2.15 g, 15.6 mmol, 1.2 eq) was added in portions and the resulting suspension was stirred until the gas evolution ceased (10 min). Then, dimethylsulfate (1.23 ml, 13 mmol, 1 eq) was added and the reaction mixture was stirred for 1 hour at room temperature. The reaction was monitored by TLC (Hexanes/AcOEt 9/1, R_{f(1)} = 0.1, R_{f(2)} = 0.7). After complete consumption of the starting material, the reaction mixture was diluted with acetone (10 ml) and filtered on a plug of celite. The solid was rinsed twice with acetone (2x10 ml) and the filtrate was concentrated using a rotary evaporator. The crude residue was triturated with hexanes (10 ml) and the resulting suspension was filtered on a plug of celite. The filtrate was concentrated using a rotary evaporator to yield the desired product as a pale yellow liquid (2.2 g, 99%). ¹H NMR (400 MHz, CDCl₃): δ 7.66-7.70 (m, 1H), 7.52-7.57 (m, 1H), 7.18-7.22 (t, *J* = 7.7 Hz, 1H), 3.84 (s, 3H), 2.26-2.27 (d, *J* = 2.4 Hz, 3H). ¹³C NMR (100 MHz, CDCl₃): δ 164.2-164.2 (d, *J* = 3.2 Hz), 158.0-160.5 (d, *J* = 256.5 Hz), 136.1-136.2 (d, *J* = 5.9 Hz), 129.1, 125.9-126.1 (d, *J* = 17.5 Hz), 124.0-124.0 (d, *J* = 4.5 Hz), 117.9-118.0 (d, *J* = 10.9 Hz), 52.3, 14.1-14.1 (d, *J* = 4.6 Hz).



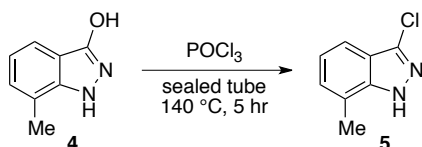
Scheme 2. Preparation of 2-fluoro-3-methylbenzohydrazide **3**.

2-fluoro-3-methylbenzohydrazide 3: methyl 2-fluoro-3-methylbenzoate **2** (2.2 g, 13 mmol, 1 eq) was charged into a 100-ml round-bottomed flask and dissolved in methanol (20 ml). Hydrazine monohydrate (3.15 ml, 65 mmol, 5 eq) was added and the flask was equipped with a reflux condenser. The flask was then placed in an oil bath preheated at 60 °C and the reaction mixture was refluxed for 1.5 hours. After this time, the reaction mixture was cooled to room temperature and volatiles were removed using a rotary evaporator. The crude residue was triturated in hexanes (20 ml) and the supernatant solution was removed with a pipet. The operation was repeated two times and the resulting gummy solid was dissolved in AcOEt, dried with Na₂SO₄, filtered and concentrated using a rotary evaporator. The crude reaction mixture was dried *in vacuo* for 12 hours to give the desired product as a white solid (1.8 g, 83%). ¹H NMR (400 MHz, d⁶-DMSO): δ 9.48 (brs, 1H), 7.32-7.40 (m, 2H), 7.12-7.15 (t, *J* = 7.6 Hz, 1H), 4.51 (brs, 2H), 2.25-2.25 (d, *J* = 2.3 Hz, 3H). ¹³C NMR (100 MHz, d⁶-DMSO): δ 163.6, 156.2-158.7 (d, *J* = 248.1 Hz), 133.2-133.3 (d, *J* = 5.2 Hz), 127.3-127.3 (d, *J* = 3.2 Hz), 124.9-125.0 (d, *J* = 17.7 Hz), 123.9-123.9 (d, *J* = 4.2 Hz), 122.9-123.1 (d, *J* = 16.1 Hz), 14.1-14.2 (d, *J* = 4.2 Hz).



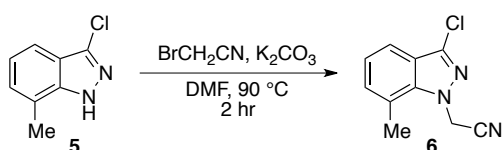
Scheme 3. Preparation of 7-methyl-1H-indazol-3-ol **4**.

7-methyl-1H-indazol-3-ol 4: 2-fluoro-3-methylbenzohydrazide **3** (1.5 g, 9 mmol, 1 eq) was charged into a sealed tube and suspended in hydrazine monohydrate (6 ml). The tube was sealed with a Teflon screw valve and placed in an oil bath preheated at 140 °C. The reaction mixture was placed behind a protective shield and stirred for 15 hours. After this time, the reaction mixture was cooled to room temperature and the protective shield was removed. The cooled mixture was poured into crushed ice and the mixture was stirred for 10 min. A white precipitate formed and was filtered off the suspension with a fritted funnel. The solid was washed twice with water (5 ml) and subsequently dried *in vacuo* for few hours to afford the desired product as a white solid (1 g, 75%). ¹H NMR (400 MHz, d⁶-DMSO): δ 10.52-11.12 (brm, 2H), 7.42-7.44 (d, *J* = 8.0 Hz, 1H), 7.07-7.09 (d, *J* = 6.9 Hz, 1H), 6.86-6.90 (dd, *J* = 6.9 and 8.0 Hz, 1H), 2.38 (s, 3H). ¹³C NMR (100 MHz, d⁶-DMSO): δ 156.6, 142.5, 127.0, 119.9, 118.9, 117.6, 112.3, 16.1.



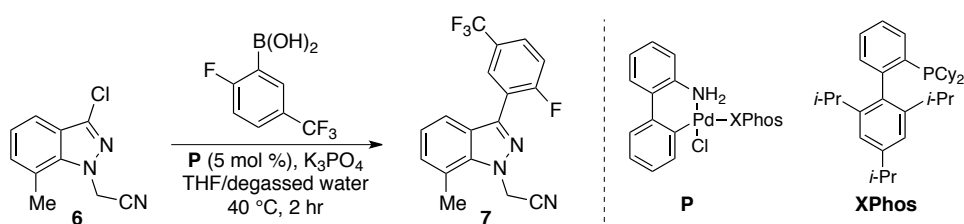
Scheme 4. Preparation of 3-chloro-7-methyl-1H-indazole **5**.

3-chloro-7-methyl-1H-indazole 5: 7-methyl-1H-indazol-3-ol **4** (500 mg, 3.38 mmol, 1 eq) was charged into a sealed tube and suspended in phosphorus (V) oxychloride (2 ml). The tube was sealed with a Teflon screw valve, placed in an oil bath preheated at 140 °C and the reaction mixture was stirred at this temperature for 5 hours. After this time, the reaction mixture was cooled to room temperature and poured into crushed ice. The mixture was stirred for 30 min and an off-white precipitate formed. The solid was filtered off the suspension with a fritted funnel. The residual water was removed by azeotropic evaporation with toluene using a rotary evaporator. The resulting solid was dried *in vacuo* for few hours to afford the desired product as an off-white solid (565 mg, 99%). ¹H NMR (400 MHz, CDCl₃): δ 7.47-7.49 (d, *J* = 8.1 Hz, 1H), 7.17-7.19 (d, *J* = 7.0 Hz, 1H), 7.09-7.13 (dd, *J* = 7.0 and 8.1 Hz, 1H), 2.53 (s, 3H). ¹³C NMR (100 MHz, CDCl₃): δ 141.6, 135.3, 128.1, 122.1, 120.7, 120.2, 117.0, 16.6.



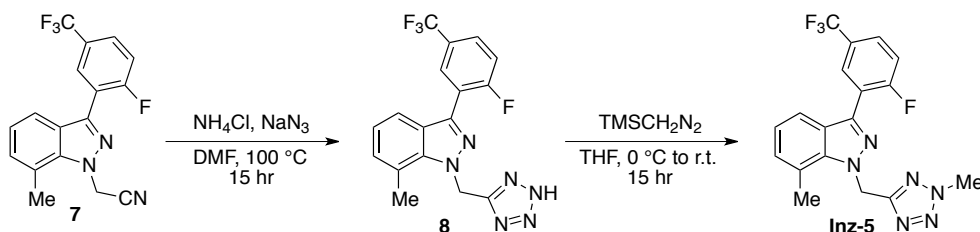
Scheme 5. Preparation of 2-(3-chloro-7-methyl-1H-indazol-1-yl)acetonitrile **6**.

2-(3-chloro-7-methyl-1H-indazol-1-yl)acetonitrile 6: 3-chloro-7-methyl-1H-indazole **5** (300 mg, 1.81 mmol, 1 eq) and potassium carbonate (500 mg, 3.62 mmol, 2 eq) were charged into a test tube and suspended in DMF (5 ml). The tube was capped with a Teflon screw-cap septum. Bromoacetonitrile (0.25 ml, 3.62 mmol, 2 eq) was added via syringe through the septum and the tube was placed in an oil bath preheated at 90 °C. The reaction was monitored by TLC (Hexanes/AcOEt 6/4, $R_{f(6)} = 0.8$). After complete consumption of the starting material (2 hours), the reaction mixture was cooled to room temperature, quenched with an aqueous solution of HCl (1M) and extracted with Et₂O. The organic layer was washed with brine, dried with Na₂SO₄, filtered and concentrated using a rotary evaporator. The crude residue was adsorbed onto silica gel, dried *in vacuo* and purified by flash chromatography (Hexanes/AcOEt 6/4, $R_{f(6)} = 0.8$) to afford the desired product as an off-white solid (350 mg, 94%). ¹H NMR (400 MHz, CDCl₃): δ 7.54-7.57 (dd, $J = 0.7, 1.3$ and 8.0 Hz, 1H), 7.26-7.28 (m, 1H), 7.17-7.21 (dd, $J = 7.1$ and 8.0 Hz, 1H), 5.43 (s, 2H), 2.79 (s, 3H). ¹³C NMR (100 MHz, CDCl₃): δ 140.8, 136.5, 130.9, 123.3, 123.2, 120.3, 118.4, 114.6, 39.9, 18.6.



Scheme 6. Preparation of 2-(3-(2-fluoro-5-(trifluoromethyl)phenyl)-7-methyl-1H-indazol-1-yl)acetonitrile **7**.

2-(3-(2-fluoro-5-(trifluoromethyl)phenyl)-7-methyl-1H-indazol-1-yl)acetonitrile 7: 2-(3-chloro-7-methyl-1H-indazol-1-yl)acetonitrile **6** (100 mg, 0.49 mmol, 1 eq), 2-fluoro-5-(trifluoromethyl)phenylboronic acid (152 mg, 0.73 mmol, 1.5 eq), tribasic potassium phosphate (212 mg, 1.0 mmol, 2 eq) and XPhos precatalyst **P** (18 mg, 0.025 mmol, 0.05 eq) were charged into a test tube, which was capped with a rubber septum. The vessel was successively evacuated and backfilled with argon. This operation was repeated three times and anhydrous THF (1 ml) was added via syringe through the septum followed by freshly degassed water (2 ml). The rubber septum was then replaced by a Teflon screw-cap septum and the tube was placed in an oil bath preheated at 40 °C. After 2 hours, the reaction mixture was cooled to room temperature, quenched with water and extracted with AcOEt. The organic layer was dried with Na₂SO₄, filtered and concentrated using a rotary evaporator. The crude residue was adsorbed onto silica gel, dried *in vacuo* and purified by flash chromatography (Hexanes/AcOEt 8/2, $R_{f(7)} = 0.5$) to afford the desired product as a yellow solid (147 mg, 90%). ¹H NMR (400 MHz, CDCl₃): δ 8.06-8.08 (dd, $J = 2.4$ and 6.4 Hz, 1H), 7.70-7.74 (m, 1H), 7.63-7.66 (dd, $J = 3.4$ and 8.1 Hz, 1H), 7.34-7.39 (m, 1H), 7.25-7.28 (m, 1H), 7.18-7.22 (dd, $J = 7.0$ and 8.1 Hz, 1H), 5.58 (s, 2H), 2.86 (s, 3H). ¹³C NMR (100 MHz, CDCl₃): δ 160.6-163.1 (d, $J = 255.6$ Hz), 141.3, 140.5, 130.1, 128.9-129.0 (m), 127.7-127.9 (m), 127.3-127.6 (m), 124.3, 123.1, 121.2-121.4 (d, $J = 16.0$ Hz), 120.1, 120.0, 119.7-127.9 (q, $J = 272.1$ Hz), 117.1-117.3 (d, $J = 23.3$ Hz), 114.9, 40.1, 18.8. ¹⁹F NMR (376 MHz, CDCl₃): δ -62.0 (s, 3F), -107.9 (s, 1F).



Scheme 7. Preparation of **Inz-5**.

3-(2-fluoro-5-(trifluoromethyl)phenyl)-7-methyl-1-((2-methyl-2H-tetrazol-5-yl)methyl)-1H-indazole Inz-5: 2-(3-(2-fluoro-5-(trifluoromethyl)phenyl)-7-methyl-1H-indazol-1-yl)acetonitrile **7** (100 mg, 0.3 mmol, 1 eq), ammonium chloride (32.4 mg, 0.6 mmol, 2 eq) and sodium azide (39 mg, 0.6 mmol, 2 eq) were charged into a test tube and suspended in DMF (1 ml). The tube was sealed with a Teflon screw-cap septum and placed in an oil bath preheated at 100 °C. The reaction mixture was stirred at this temperature for 15 hours. After this time, the reaction mixture was cooled to room temperature, quenched with an aqueous solution of HCl (1M) and extracted with Et₂O. The organic layer was dried with Na₂SO₄, filtered and concentrated using a rotary

evaporator to recover compound **8** as a yellow oil. The crude mixture (100 mg, 0.27 mmol, 1 eq) was charged into a test tube, which was subsequently closed with a Teflon screw-cap septum. The vessel was successively evacuated and backfilled with argon. This operation was repeated three times and anhydrous THF (2 ml) was added via syringe through the septum. The reaction mixture was cooled to 0 °C with an ice bath and a solution of (trimethylsilyl)diazomethane in hexanes (2M, 0.2 ml, 0.41 mmol, 1.5 eq) was added dropwise via syringe through the septum. Then, the ice bath was removed and the yellow reaction mixture was stirred for 15 hours. After this time, the excess (trimethylsilyl)diazomethane was quenched with few drops of tetrafluoroboric acid. When the gas evolution ceased, the reaction mixture was concentrated using a rotary evaporator. The crude residue was adsorbed onto silica gel, dried *in vacuo* and purified by flash chromatography (Hexanes/AcOEt 6/4, R_f(_{lnz-5}) = 0.7) to afford the desired product as a white solid (23 mg, 22% from **8**). **¹H NMR (400 MHz, CDCl₃)**: δ 8.06-8.08 (dd, *J* = 2.1 and 6.4 Hz, 1H), 7.65-7.69 (m, 1H), 7.59-7.62 (dd, *J* = 3.3 and 8.0 Hz, 1H), 7.30-7.35 (appt, *J* = 9.1 Hz, 1H), 7.18-7.20 (dt, *J* = 1.2 and 6.9 Hz, 1H), 7.11-7.14 (dd, *J* = 7.0 and 8.1 Hz, 1H), 6.14 (s, 2H), 4.28 (s, 3H), 2.83 (s, 3H). **¹³C NMR (100 MHz, CDCl₃)**: δ 163.4, 160.6-163.2 (d, *J* = 256.0 Hz), 140.6, 139.9, 129.3, 129.1-129.3 (m), 127.0-127.4 (m, 2C), 123.8, 119.8-127.9 (q, *J* = 272.2 Hz), 122.2, 122.0-122.1 (d, *J* = 16.1 Hz), 120.7, 119.5-119.6 (d, *J* = 7.2 Hz), 116.8-117.1 (d, *J* = 23.5 Hz), 46.8, 39.7, 19.4. **¹⁹F NMR (376 MHz, CDCl₃)**: δ -61.9 (s, 3F), -108.0 (s, 1F). **LC-MS**: R_T = 2.3 min (>98% purity). **HRMS (*m/z*)**: [M+H] calculated for C₁₈H₁₅F₄N₆, 391.1289; found, 391.1277.

Comment: The low isolated yield obtained after the methylation step was due to the concomitant formation of a regioisomer, which was separated during the purification by flash chromatography. The identity of each regioisomer and notably the position of the methyl group were ascertained by 2D NMR experiments (HMBC and HSQC).²

Supplemental References

- Altman, M.D., Ali, A., Reddy, G.S., Nalam, M.N., Anjum, S.G., Cao, H., Chellappan, S., Kairys, V., Fernandes, M.X., Gilson, M.K., *et al.* (2008). HIV-1 protease inhibitors from inverse design in the substrate envelope exhibit subnanomolar binding to drug-resistant variants. *Journal of the American Chemical Society* *130*, 6099-6113.
- Huggins, D.J., Altman, M.D., and Tidor, B. (2009). Evaluation of an inverse molecular design algorithm in a model binding site. *Proteins* *75*, 168-186.
- Kinzel, T., Zhang, Y., and Buchwald, S.L. (2010). A New Palladium Precatalyst Allows for the Fast Suzuki-Miyaura Coupling Reactions of Unstable Polyfluorophenyl and 2-Heteroaryl Boronic Acids. *J Am Chem Soc* *132*, 14073-14075.
- Vincent, B.M., Lancaster, A.K., Scherz-Shouval, R., Whitesell, L., and Lindquist, S. (2013). Fitness trade-offs restrict the evolution of resistance to amphotericin B. *PLoS biology* *11*, e1001692.